

Landau fluids for space plasmas

T. Passot et P.L. Sulem
Observatoire de la Côte d'Azur, Nice

Nonlinear structures in the form of **magnetic holes** anti-correlated with the **plasma density** and propagating very slowly in directions almost **transverse** to the ambient field. They are observed in the magnetosheath and result from the growth of **mirror modes** that are unstable in regions with a **high β** and a **strong proton temperature anisotropy**.

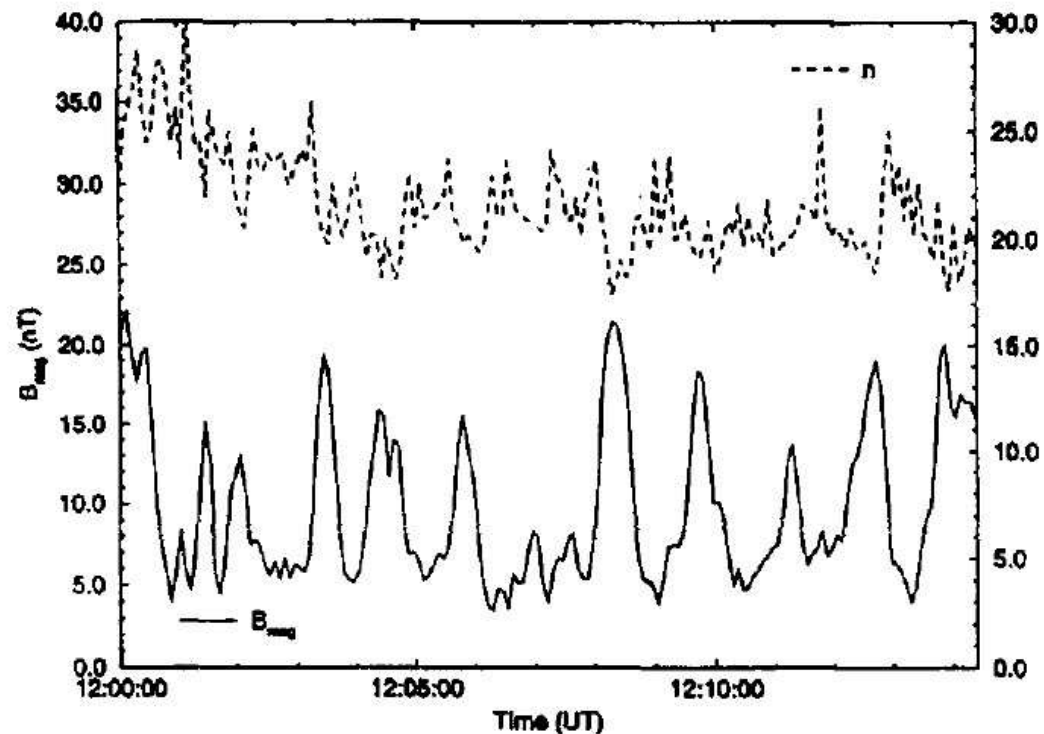


Figure 1: From Leckband et al. (1995), Adv. Space Res. **15**, 345.

Mirror bubbles with broad troughs and steep walls.
Quasi-perpendicular propagation

Density is anti-correlated

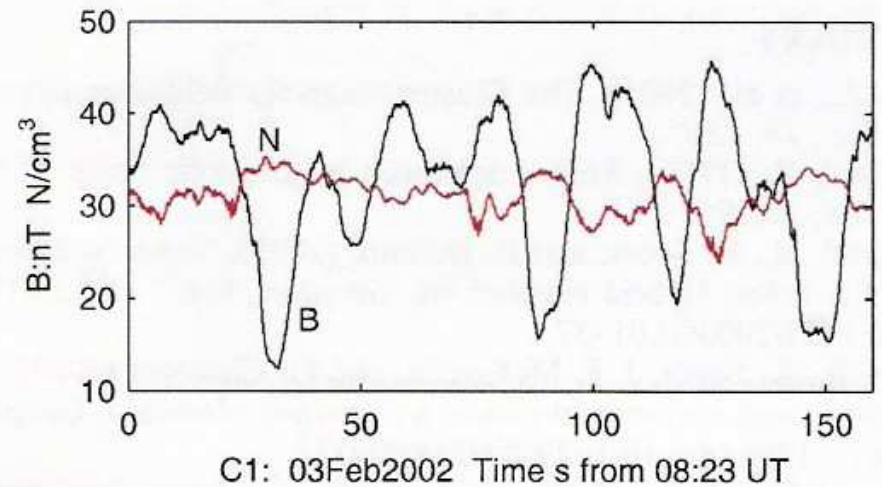
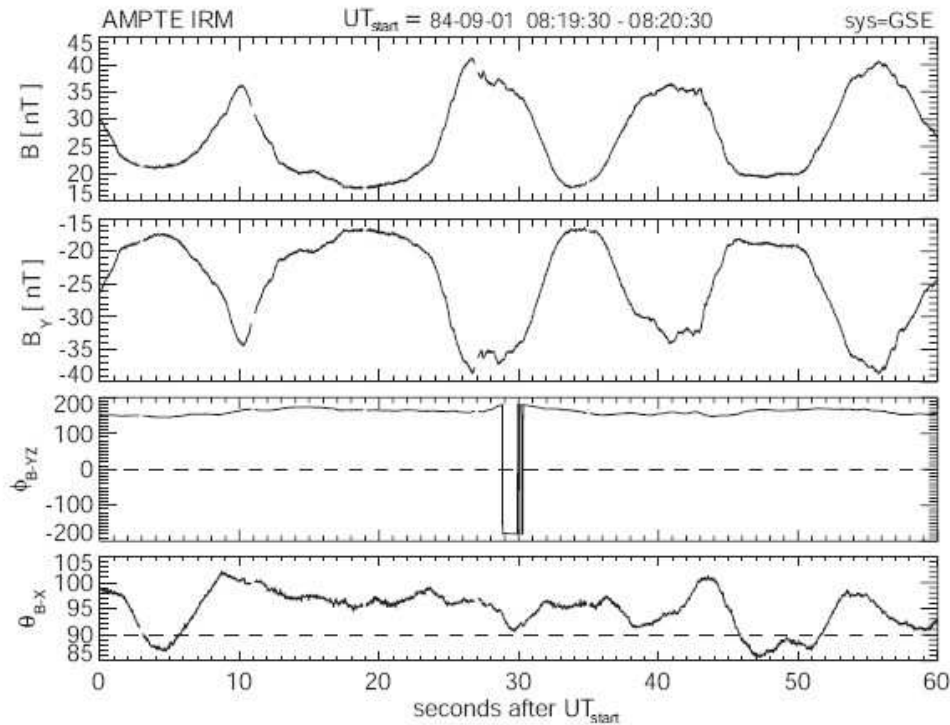


Figure 2:

Left: from Treumann et al. (2004), NPG **11**, 647.;

Right: from Stasiewicz (2004), GRL **31**, L21804.

Filaments

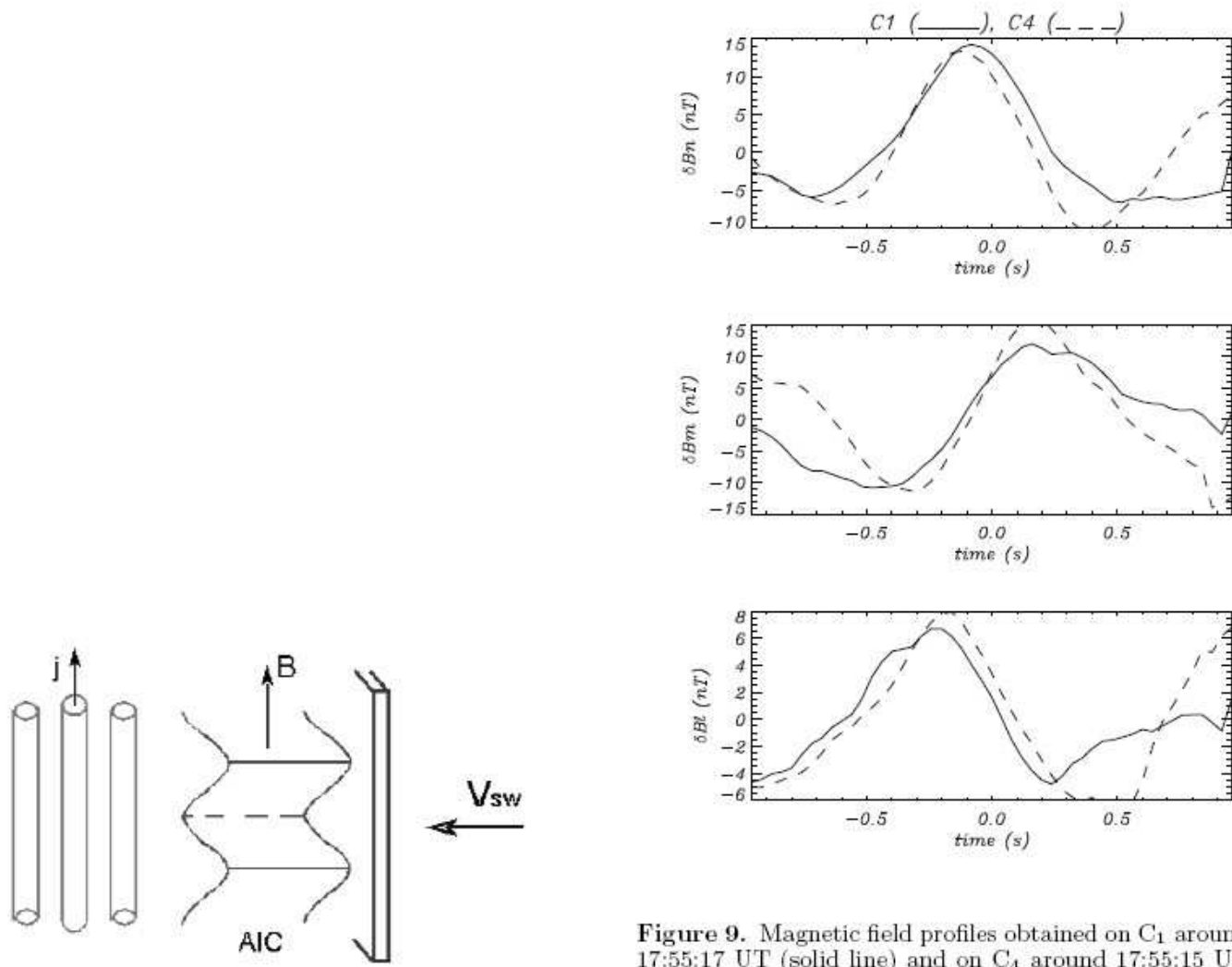


Figure 9. Magnetic field profiles obtained on C₁ around 17:55:17 UT (solid line) and on C₄ around 17:55:15 UT (dashed line).

Figure 3: From Alexandrova et al. (2004), JGR **109**, A05207.

Cluster spacecrafts allow one to **determine k -spectra and clearly identify modes**. For the first time a turbulent spectra of **nonlinearly interacting mirror modes** has been identified (Sahraoui et al. 2005).

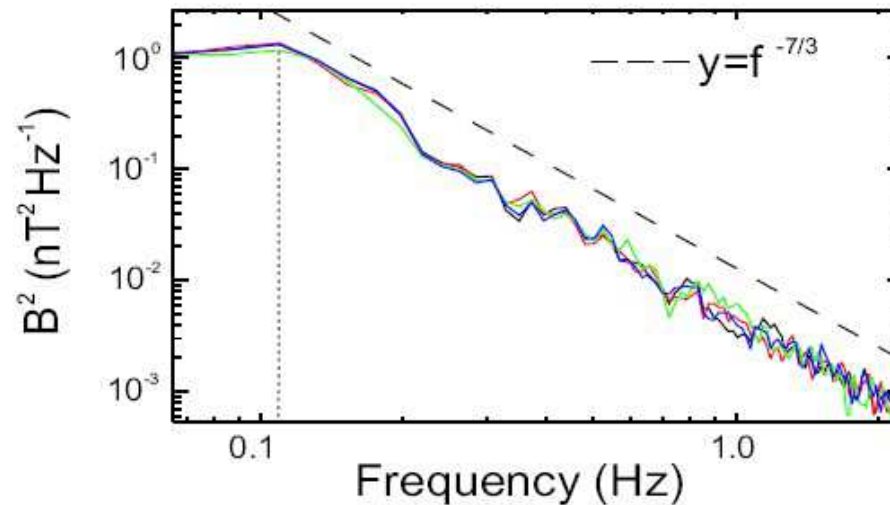


Figure 4: Sahraoui et al. (2003) JGR **108**, A9, SMP1,1-18.

Magnetosheath displays a **wide spectrum of low frequency modes** (Alfvén, slow and fast magnetosonic, mirror).

Size of perturbations can be **smaller than the ion gyroradius**.

The plasma is **warm and collisionless**.

Landau damping and finite Larmor radius corrections play an important role.

The origin of **coherent solitonic structures** (magnetic holes and shocklets) is still debated (Tsurutani et al. 2004). The spectra are also unexplained.

One needs simulation of this medium with a large range of scales.

Which tool?

- Description of intermediate-scale dynamics by usual MHD is questionable.
- Numerical integration of Vlasov-Maxwell or gyrokinetic equations often beyond the capabilities of present day computers.
- Need for a reduced description that retains most of the aspects of a FLUID MODEL but INCLUDES REALISTIC APPROXIMATIONS OF THE PRESSURE TENSOR AND WAVE-PARTICLE RESONANCES.

Should remain simple enough to allow 3D numerical simulations of turbulent regime.

★ **Gyrofluids**: hydrodynamic moments obtained from gyrokinetic equations. Capture high order FLR corrections but need a specific closure and are written in a local reference frame.

★ **Landau fluids** [Hammett and co-authors (1990s)]: monofluid taking into account wave-particle resonances in a way consistent with linear kinetic theory.

Landau fluids for dispersive MHD: outline of the method

- Goal: Extend Landau-fluid model, to reproduce the weakly nonlinear dynamics of dispersive MHD (magnetosonic and Alfvén) waves whatever their direction of propagation, in particular of kinetic Alfvén waves (KAW) with $k\rho_L \leq 1$, by retaining FLR corrections and a generalized Ohm's law in addition to Landau damping.
- Starting point: Vlasov-Maxwell (VM) equations.
- Small parameter: ratio between the ion Larmor radius and the typical (smallest) wavelength. Field amplitudes also supposed to be small.
- Main problem: Exact hydrodynamic equations are obtained by taking moments of VM equations. The hierarchy must however be closed and the main work resides in a proper determination of the pressure tensor.
- Assumptions: Homogeneous equilibrium state with bi-Maxwellian distribution functions.

Basic tensors

$$\boldsymbol{\tau} = \hat{\mathbf{b}} \otimes \hat{\mathbf{b}} \quad \mathbf{n} = \mathbf{I} - \boldsymbol{\tau} \quad \text{where} \quad \hat{\mathbf{b}} = \mathbf{b}/B_0$$

Pressure tensor $\mathbf{p} = \mathbf{P} + \boldsymbol{\Pi}$ sum of a gyrotropic pressure $\mathbf{P} = p_{\perp} \mathbf{n} + p_{\parallel} \boldsymbol{\tau}$ (with $2p_{\perp} = \mathbf{p} : \mathbf{n}$ and $p_{\parallel} = \mathbf{p} : \boldsymbol{\tau}$) and of a gyroviscosity tensor $\boldsymbol{\Pi}$ that satisfies $\boldsymbol{\Pi} : \mathbf{n} = 0$ and $\boldsymbol{\Pi} : \boldsymbol{\tau} = 0$.

Similar decomposition of the heat flux tensor $\mathbf{q} = \mathbf{S} + \boldsymbol{\sigma}$ with the conditions $\sigma_{ijk} n_{jk} = 0$ and $\sigma_{ijk} \tau_{jk} = 0$. The tensor $\boldsymbol{\sigma}$ can be neglected.

We thus characterize \mathbf{q} by the **parallel and transverse heat flux vectors** S^{\parallel} and S^{\perp} with components $S_i^{\parallel} = q_{ijk} \tau_{jk}$ and $2S_i^{\perp} = q_{ijk} n_{jk}$.

Since $m_e/m_i \ll 1$: **only non-gyrotropic corrections due to ions are retained.**

Weakly nonlinear regime: **nongyrotropic contributions $\boldsymbol{\Pi}$, S_{\perp}^{\perp} and S_{\perp}^{\parallel} retained at the linear level only.**

Equations for the **gyrotropic pressure components**,

$$\begin{aligned} \partial_t p_{\perp} + \nabla \cdot (u p_{\perp}) + p_{\perp} \nabla \cdot u - p_{\perp} \hat{b} \cdot \nabla u \cdot \hat{b} + \frac{1}{2} (\text{tr} \nabla \cdot \mathbf{q} - \hat{b} \cdot (\nabla \cdot \mathbf{q}) \cdot \hat{b}) \\ + \frac{1}{2} (\text{tr} (\mathbf{\Pi} \cdot \nabla u)^S - (\mathbf{\Pi} \cdot \nabla u)^S : \boldsymbol{\tau} + \mathbf{\Pi} : \frac{d\boldsymbol{\tau}}{dt}) = 0 \\ \partial_t p_{\parallel} + \nabla \cdot (u p_{\parallel}) + 2p_{\parallel} \hat{b} \cdot \nabla u \cdot \hat{b} + \hat{b} \cdot (\nabla \cdot \mathbf{q}) \cdot \hat{b} + (\mathbf{\Pi} \cdot \nabla u)^S : \boldsymbol{\tau} - \mathbf{\Pi} : \frac{d\boldsymbol{\tau}}{dt} = 0. \end{aligned}$$

Total energy is **conserved** whatever the form of $\mathbf{\Pi}$ and the closure relations.

In the case where the distribution function is close to a **Maxwellian**, the fourth order moment is conveniently written in the form

$$\begin{aligned} \rho r_{ijkl} = & P_{ij}P_{lk} + P_{ik}P_{jl} + P_{il}P_{jk} + P_{ij}\Pi_{lk} + P_{ik}\Pi_{jl} + P_{il}\Pi_{jk} \\ & + \Pi_{ij}P_{lk} + \Pi_{ik}P_{jl} + \Pi_{il}P_{jk} + \rho \tilde{r}_{ijkl}. \end{aligned}$$

with a **gyrotropic form** for the tensor \tilde{r} :

$$\begin{aligned} \tilde{r}_{ijkl} = & \frac{\tilde{r}_{\parallel\parallel\parallel}}{3} (\tau_{ij}\tau_{kl} + \tau_{ik}\tau_{jl} + \tau_{il}\tau_{jk}) + \tilde{r}_{\parallel\perp} (n_{ij}\tau_{kl} + n_{ik}\tau_{jl} + n_{il}\tau_{jk} \\ & + \tau_{ij}n_{kl} + \tau_{ik}n_{jl} + \tau_{il}n_{jk}) + \frac{\tilde{r}_{\perp\perp}}{2} (n_{ij}n_{kl} + n_{ik}n_{jl} + n_{il}n_{jk}) \end{aligned}$$

$$\nabla_{\perp} \cdot \Pi_{\perp} = \frac{p_{\perp}^{(0)}}{2\Omega} \hat{z} \times \Delta_{\perp} u - \frac{\rho^{(0)}}{2m} r_L^2 \Delta_{\perp} \nabla_{\perp} T_{\perp}^{(1)} - \frac{1}{2\Omega^2} \Delta_{\perp} \nabla_{\perp} \tilde{r}_{\perp\perp} + \frac{1}{2\Omega} \hat{z} \times \partial_t \nabla_{\perp} \cdot \Pi_{\perp}$$

$$S_{\perp}^{\perp} = \frac{2p_{\perp}^{(0)}}{m\Omega} \hat{z} \times \nabla_{\perp} T_{\perp}^{(1)} - \frac{p_{\perp}^{(0)}}{2} r_L^2 \Delta_{\perp} u_{\perp} + \frac{2}{\Omega} \hat{z} \times \nabla_{\perp} \tilde{r}_{\perp\perp} + \frac{1}{\Omega} \hat{z} \times \partial_t S_{\perp}^{\perp}$$

$$\Pi_z = \frac{\hat{z}}{\Omega} \times (\nabla_{\perp} S_z^{\perp} + p_{\perp}^{(0)} \nabla_{\perp} u_z + p_{\parallel}^{(0)} \partial_z u_{\perp} - (p_{\perp}^{(0)} - p_{\parallel}^{(0)}) \partial_t \hat{b}_{\perp} + \partial_t \Pi_z)$$

$$- \frac{1}{\Omega^2} \partial_z \left(\frac{p_{\perp}^{(0)}}{m} \nabla_{\perp} T_{\parallel}^{(1)} - 2 \frac{p_{\perp}^{(0)} - p_{\parallel}^{(0)}}{m} T_{\parallel}^{(0)} \partial_z \hat{b}_{\perp} + \nabla_{\perp} \tilde{r}_{\parallel\perp} \right)$$

$$S_{\perp}^{\parallel} = \frac{\hat{z}}{\Omega} \times \left(\frac{p_{\perp}^{(0)}}{m} \nabla_{\perp} T_{\parallel}^{(1)} - 2 \frac{p_{\perp}^{(0)} - p_{\parallel}^{(0)}}{m} T_{\parallel}^{(0)} \partial_z \hat{b}_{\perp} + \nabla_{\perp} \tilde{r}_{\parallel\perp} + \partial_t S_{\perp}^{\parallel} \right)$$

$$- \frac{2T_{\parallel}^{(0)}}{m\Omega^2} \partial_z (\nabla_{\perp} S_z^{\perp} + p_{\perp}^{(0)} \nabla_{\perp} u_z + p_{\parallel}^{(0)} \partial_z u_{\perp} - (p_{\perp}^{(0)} - p_{\parallel}^{(0)}) \partial_t \hat{b}_{\perp}).$$

$$\nabla_{\perp} \cdot \Pi_{\perp} = (\partial_x \Pi_{xx} + \partial_y \Pi_{xy}, \partial_x \Pi_{xy} + \partial_y \Pi_{yy}, 0),$$

$$\Pi_z = (\Pi_{xz}, \Pi_{yz}, \Pi_{zz} = 0).$$

Nonlinear equations for the longitudinal components of parallel and transverse heat flux vectors (retaining only lowest order nonlinearities)

$$\begin{aligned} & \partial_t S_z^{\parallel} + \nabla \cdot (S_z^{\parallel} u) + 3S_z^{\parallel} \partial_z u_z + 3p_{\parallel} (\hat{b} \cdot \nabla) \left(\frac{p_{\parallel}}{\rho} \right) - p_{\perp}^{(0)} \hat{b}_{\perp} \cdot \nabla_{\perp} \left(\frac{p_{\parallel}}{\rho} \right) \\ & + \frac{2p_{\parallel}^{(0)}}{\rho^{(0)}} (p_{\parallel}^{(0)} - p_{\perp}^{(0)}) \partial_z \hat{b}_z + \nabla \cdot (\tilde{r}_{\parallel\parallel} \hat{b}) - 3\tilde{r}_{\parallel\perp} \nabla \cdot \hat{b} - (b_{\perp} \cdot \nabla_{\perp}) \tilde{r}_{\parallel\perp} = 0, \end{aligned}$$

$$\begin{aligned} & \partial_t S_z^{\perp} + \nabla \cdot (u S_z^{\perp}) + S_z \nabla \cdot u + p_{\parallel} (\hat{b} \cdot \nabla) \left(\frac{p_{\perp}}{\rho} \right) - 2p_{\perp}^{(0)} (\hat{b}_{\perp} \cdot \nabla_{\perp}) \left(\frac{p_{\perp}}{\rho} \right) \\ & + \frac{p_{\perp}^{(0)}}{\rho^{(0)}} (\partial_x \Pi_{xz} + \partial_y \Pi_{yz}) + \nabla \cdot (\tilde{r}_{\parallel\perp} \hat{b}) \\ & + \left(\frac{p_{\perp} (p_{\parallel} - p_{\perp})}{\rho} - \tilde{r}_{\perp\perp} + \tilde{r}_{\parallel\perp} \right) (\nabla \cdot \hat{b}) - (\hat{b}_{\perp} \cdot \nabla_{\perp}) \tilde{r}_{\perp\perp} = 0. \end{aligned}$$

Fourth order moment closure

Turn to kinetic theory. Compute various hydrodynamic quantities using linearly perturbed distribution function, at second order in ω/Ω .

When comparing $\tilde{r}_{\parallel\parallel\parallel}$ with S_z^{\parallel} or $T_{\parallel}^{(1)}$, one gets ($\zeta = \frac{\omega}{|k_{\parallel}|} \sqrt{\frac{m}{2T_{\parallel}^{(0)}}}$).

$$\tilde{r}_{\parallel\parallel\parallel} = \sqrt{\frac{2T_{\parallel}^{(0)}}{m}} \frac{2\zeta^2(1 + 2\zeta^2 R(\zeta)) + 3(R(\zeta) - 1) - 12\zeta^2 R(\zeta)}{2\zeta(1 - 3R(\zeta) + 2\zeta^2 R(\zeta))} S_z^{\parallel}.$$

$$\tilde{r}_{\parallel\parallel\parallel} = \frac{p_{\parallel}^{(0)} T_{\parallel}^{(0)}}{m} \frac{2\zeta^2(1 + 2\zeta^2 R(\zeta)) + 3(R(\zeta) - 1) - 12\zeta^2 R(\zeta)}{1 - R(\zeta) + 2\zeta^2 R(\zeta)} \frac{T_{\parallel}^{(1)}}{T_{\parallel}^{(0)}}.$$

Proceeding as in Snyder et al. (1997), we write

$$\tilde{r}_{\parallel\parallel\parallel} = \beta_{\parallel} p_{\parallel}^{(0)} \frac{T_{\parallel}^{(0)}}{m} \left[\frac{T_{\parallel}^{(1)}}{T_{\parallel}^{(0)}} - D_{\parallel} \sqrt{\frac{2T_{\parallel}^{(0)}}{m}} i \frac{k_z}{|k_z|} S_z^{\parallel} \right],$$

where $\beta_{\parallel} = \frac{32-9\pi}{3\pi-8}$ and $D_{\parallel} = \frac{2\sqrt{\pi}}{3\pi-8}$ are determined by matching with the exact kinetic expressions in the isothermal $|\zeta| \ll 1$ and adiabatic limits $|\zeta| \gg 1$.

A similar method leads to a dynamical equation for $\tilde{r}_{\parallel\perp}$

$$\left(\frac{d}{dt} - \frac{2}{\sqrt{\pi}} \sqrt{\frac{2T_{\parallel}^{(0)}}{m}} \mathcal{H}_z \partial_z \right) \tilde{r}_{\parallel\perp} + \frac{2T_{\parallel}^{(0)}}{m} \partial_z [S_z^{\perp} + \frac{p_{\perp}^{(0)}}{v_A^2} \left(\frac{T_{\perp}^{(0)} - T_{\parallel}^{(0)}}{m_p} \right) \frac{j_z}{en^{(0)}}] = 0.$$

$\tilde{r}_{\perp\perp}$ negligible in the large scale limit.

Validation

- For parallel Alfvén waves,
Leading order (proton) gyroviscous tensor is sufficient

$$\begin{aligned}\pi_{xx}^{(1)} = -\pi_{yy}^{(1)} &= -\frac{p_{\perp}}{2\Omega}(\partial_y u_x + \partial_x u_y), & \pi_{zz}^{(1)} &= 0, & \pi_{xy}^{(1)} &= -\frac{p_{\perp}}{2\Omega}(\partial_y u_y - \partial_x u_x) \\ \pi_{yz}^{(1)} &= \frac{1}{\Omega}[2p_{\parallel}\partial_z u_x + p_{\perp}(\partial_x u_z - \partial_z u_x)], & \pi_{xz}^{(1)} &= -\frac{1}{\Omega}[2p_{\parallel}\partial_z u_y + p_{\perp}(\partial_y u_z - \partial_z u_y)]\end{aligned}$$

Only the longitudinal components S_z^{\perp} and S_z^{\parallel} of the transverse and parallel heat transfer vectors are relevant.

The long-wave reductive perturbative expansion performed on the resulting Landau-fluid model reproduces the **KDNLS equation** derived from Vlasov-Maxwell, up to the replacement of the plasma response functions by the corresponding two- or four-pole approximants.

Consequence: modulational type instabilities (including filamentation) of Alfvén waves and their weakly nonlinear developments are correctly reproduced.

DECAY INSTABILITY:

Forward Alfvén wave \rightarrow forward acoustic wave + backward Alfvén wave with a wavenumber smaller than that of the pump.

An **algebraic inverse cascade** develops: EXCITATION IS TRANSFERRED TO LARGER AND LARGER SCALES WHILE THE DIRECTION OF PROPAGATION OF THE WAVE SWITCHES ALTERNATIVELY AT EACH STEP OF THE PROCESS.

Each step is associated with a **parallel ion temperature increase**.

Electrons remain cold. Results are in good agreement with Vasquez (1995).

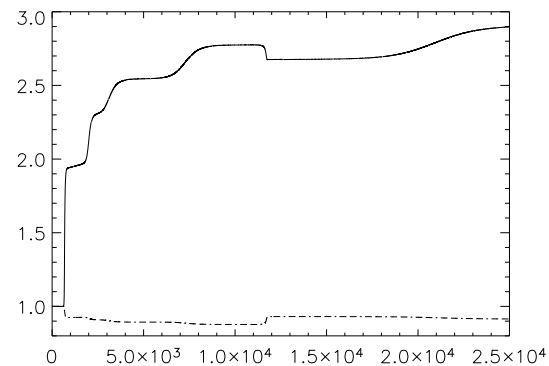


Figure 5: Ion temperature evolution for a run with a right-handed wave with amplitude $b_0 = 0.5$, in a plasma with $\beta = 0.45$ and $T_e = 0$.

Decay instability can persist at high values of β .

Taking $R_p = \frac{v_A}{\Omega_p L_0} = 0.1$ (ratio of proton inertial length scale to reference length scale), $b_0 = 0.5$ and $\beta = 5$, a decay instability is visible at early time whereas fluid theory predicts a modulational instability.

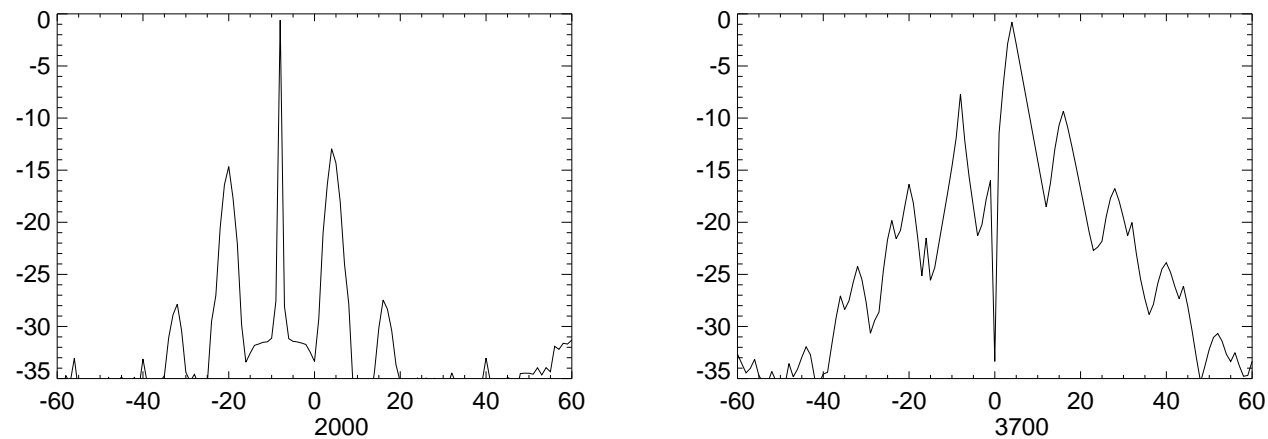


Figure 6: Spectral density for the complex quantity $b_+ = b_x + ib_y$ in the linear phase of the decay instability at $t = 2000$ (left) and in the nonlinear phase at $t = 3700$ (right) for the run with a right-hand polarized wave with amplitude $b_0 = 0.5$, in a plasma with $\beta = 5$, $R_p = 0.1$ and $T_i/T_e = 1.5$.

Mirror modes

Although **particle trapping** certainly plays a role in the saturation of the mirror instability, it is of interest to focus on the role of **hydrodynamic nonlinearities** that may be at the origin of the observed turbulent spectra.

In the quasi-hydrodynamic approach, the maximum growth rate is proportional to k_{\perp} , whereas **kinetic theory predicts the quenching of the instability for perpendicular scales of the order of the ion Larmor radius** (Pokhotelov et al. 2004, JGR **109**, A09213).

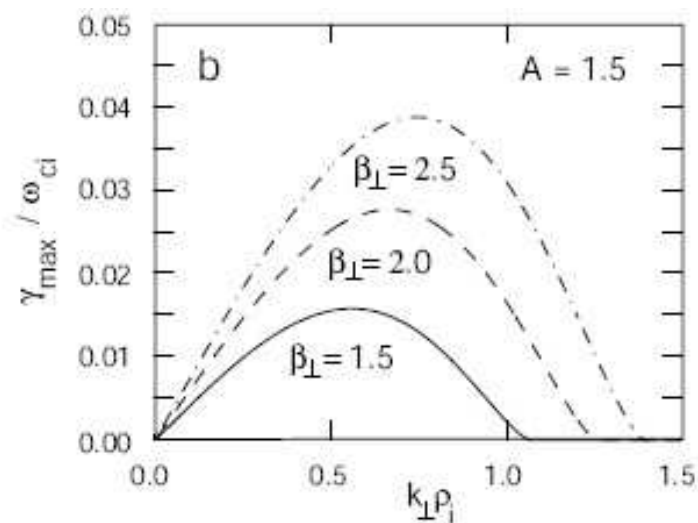


Figure 7: Growth rate of the mirror instability, maximized over the propagation angle, as a function of transverse wavenumber, from above reference.

We here present a Landau fluid model that extends MHD equations by including finite Larmor radius (FLR) corrections which is capable to accurately reproduce the dynamics of mirror modes, including at scales close to the ion Larmor radius.

Fluid model

$$\partial_t \rho_p + \nabla \cdot (\rho_p u_p) = 0$$

$$\partial_t u_p + u_p \cdot \nabla u_p + \frac{1}{\rho_p} \nabla \cdot \mathbf{p}_p - \frac{e}{m_p} \left(E + \frac{1}{c} u_p \times B \right) = 0$$

$$E = -\frac{1}{c} \left(u_p - \frac{j}{ne} \right) \times B - \frac{1}{ne} \nabla \cdot \mathbf{p}_e,$$

together with Maxwell's equations. The ion pressure tensor is rewritten as the sum $\mathbf{p}_p = p_{\perp p} (\mathbf{I} - \hat{b} \otimes \hat{b}) + p_{\parallel p} \hat{b} \otimes \hat{b} + \mathbf{\Pi}$ of the gyrotropic and gyroviscous contributions, while the electron pressure is taken gyrotropic.

One then needs to rewrite the pressure tensor, as obtained by kinetic theory, in terms of fluid quantities, thus eliminating the dependence on the plasma response function.

In order to have a description that is consistent with the linear kinetic theory, we are here led to prescribe, assuming a **regime close to isothermality**,

$$T_{\parallel r} = T_{\parallel r}^{(0)} (1 + \alpha_{\parallel r})$$

$$T_{\perp r} = T_{\perp r}^{(0)} \left(\frac{|B|}{B_0} \right)^{-A_r} (1 + \alpha_{\perp r}).$$

A matching with kinetic theory leads us to prescribe $\alpha_{\parallel p}$ as the solution of the **dynamical equation**

$$\left(\partial_t - \frac{2}{\sqrt{\pi}} \sqrt{\frac{2T_{\parallel p}^{(0)}}{m_p}} \mathcal{H}_z \partial_z \right) \alpha_{\parallel p} + 2 \partial_z \left[u_{zp} + \frac{T_{\perp p}^{(0)} - T_{\parallel p}^{(0)}}{m_p} \frac{1 - \Gamma_0(b)}{b} \frac{1}{v_A^2} \frac{j_z}{en^{(0)}} \right] = 0$$

with similar equations for the other quantities.

Modelization of the gyroviscous stress

We write

$$\frac{1}{p_{\perp p}^{(0)}} \nabla_{\perp} \cdot \mathbf{\Pi}_{\perp} = -\nabla_{\perp} \mathcal{A} + \nabla_{\perp} \times (\mathcal{B} \hat{z}).$$

After various substitutions in the kinetic expression of \mathcal{A} and \mathcal{B} , one obtains

$$\mathcal{A} = \left(1 - \frac{\Gamma_1(b)}{b[\Gamma_0(b) - \Gamma_1(b)]} + \frac{\Gamma_1(b)}{\Gamma_0(b)}\right) \frac{i(k_{\perp} \times u_{\perp p}) \cdot \hat{z}}{\Omega} - \frac{\Gamma_1(b)}{\Gamma_0(b)} \frac{T_{\perp p}^{(1)}}{T_{\perp p}^{(0)}}$$

$$\begin{aligned} \mathcal{B} = & -i \frac{\omega}{\Omega} \left[\frac{\Gamma_0(b) - 1 - \Gamma_1(b)}{b} + 2(\Gamma_0(b) - \Gamma_1(b)) + \frac{\Gamma_0(b) - \Gamma_1(b)}{1 - \Gamma_0(b)} (\Gamma_0(b) - \Gamma_1(b) - \frac{1 - \Gamma_0(b)}{b}) \right] \frac{b_z}{B_0} \\ & + \frac{1}{1 - \Gamma_0(b)} \left[\Gamma_0(b) - \Gamma_1(b) - \frac{1 - \Gamma_0(b)}{b} \right] \frac{i(k_{\perp} \cdot u_{\perp p})}{\Omega}. \end{aligned}$$

Let us now turn to $\Pi_z = (\Pi_{xz}, \Pi_{yz}, \Pi_{zz})$ where $\Pi_{zz} = 0$.

This vector was neglected by Smolyakov et al. (1995) and Cheng and Johnson (1999), but turns out not to be globally negligible. Writing

$$\Pi_z = -\nabla_{\perp} \mathcal{C} + \nabla_{\perp} \times (\mathcal{D} \hat{z}),$$

simplified expressions for \mathcal{C} and \mathcal{D} can be derived from kinetic theory

$$\frac{\mathcal{C}}{p_{\parallel p}^{(0)}} = i \frac{k_z}{k_{\perp}^2} \left(\frac{T_{\perp}^{(0)}}{T_{\parallel}^{(0)}} - 1 \right) \left[(\Gamma_0(b) - \Gamma_1(b) - 1) \frac{b_z}{B_0} - (1 - \Gamma_0(b)) \frac{e\Psi}{T_{\perp}^{(0)}} \right]$$

$$\frac{\mathcal{D}}{p_{\parallel p}^{(0)}} = (\Gamma_0(b) - \Gamma_1(b) - 1) \left(\frac{T_{\perp}^{(0)}}{T_{\parallel}^{(0)}} - 1 \right) \frac{4\pi}{cB_0 k_{\perp}^2} j_z.$$

Comparison with kinetic theory

Linearization of the fluid model leads to a dispersion relation whose solutions can be compared to those of the kinetic theory.

Dispersion relation of KAWs

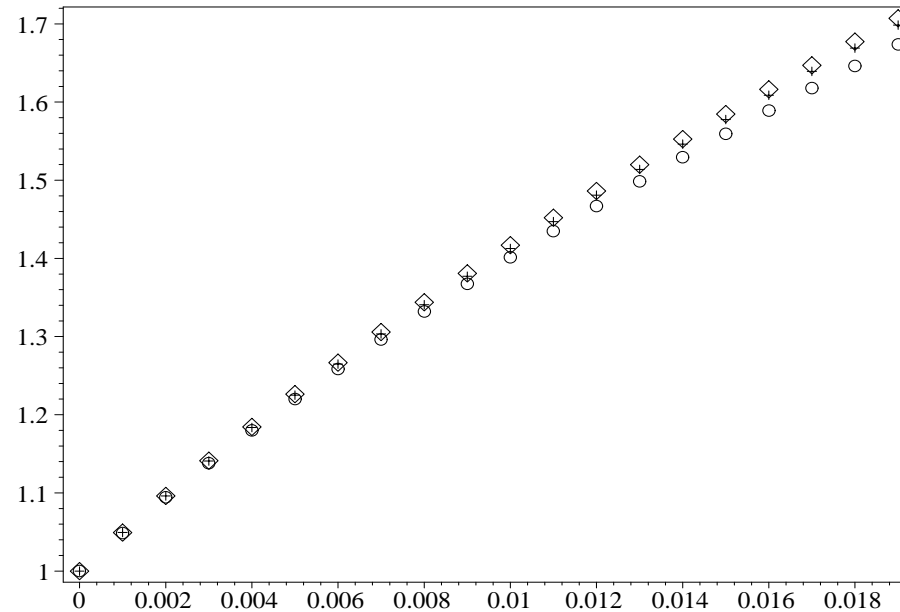


Figure 8: Comparison of the normalized frequencies $\Re(\omega)/k_z v_A$ of kinetic Alfvén waves as a function of b for $\beta_{\perp p} = 0.001$, $\tau = 100$ and isotropic equilibrium temperatures, obtained by numerical resolution of the full dispersion relation (circles) and from the analytic formula $\omega^2 = k_z^2 v_A^2 (1 + (\frac{3}{4} + \frac{T_e^{(0)}}{T_p^{(0)}})b)$ (diamonds). The cross symbols refer to the predictions of the fluid model.

COMPARISON WITH THE LINEAR THEORY OF MIRROR MODES

Close to threshold

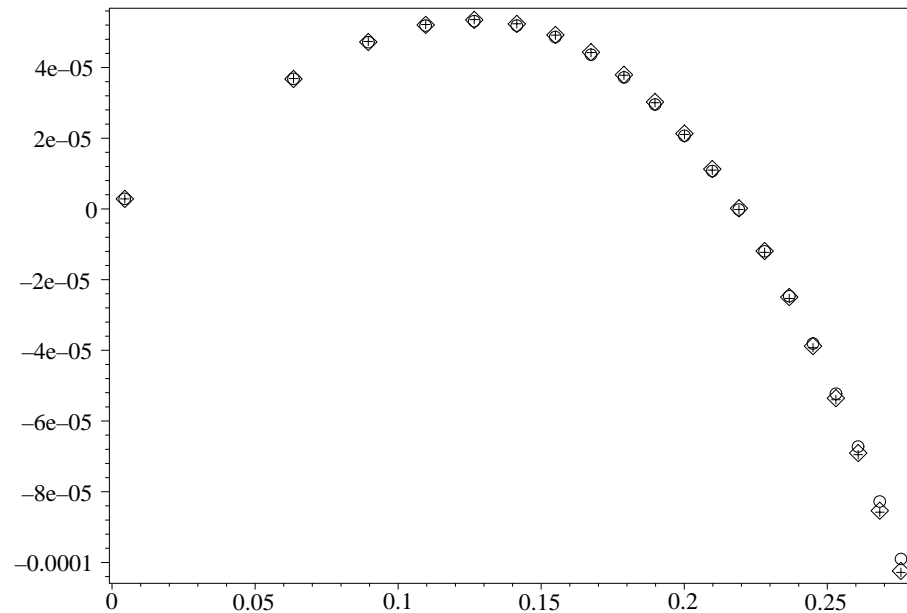


Figure 9: Growth rates γ/Ω as a function of $k_{\perp} r_p = \sqrt{2b}$ for $\tau = 0$, $A_p = 0.7$, $\beta_{\perp p} = 1.5$, $\theta = 0.1$ obtained from kinetic theory (diamonds) and the fluid model (circles). Crosses correspond to an extended version of the model.

Further away from threshold

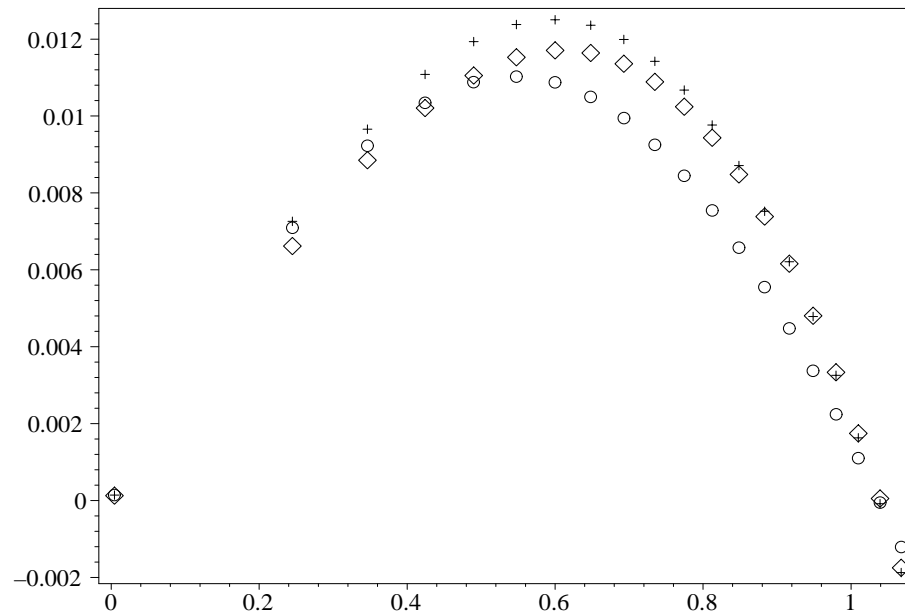


Figure 10: Growth rates γ/Ω as a function of $k_{\perp} r_p = \sqrt{2b}$ for $\tau = 1$, $A_p = 1.5$, $A_e = 0.1$, $\beta_{\perp p} = 1.5$, $\theta = 0.2$ obtained from kinetic theory (diamonds) and the fluid model (circles). Crosses correspond to a linear model where all terms are kept in the FLR corrections and a fourth pole approximation is used for the plasma response function in the first term of Π_{yz} .

Alfvén wave filamentation

Self-focusing instability

In the context of Hall-MHD

Whatever their polarization, monochromatic Alfvén waves are unstable relatively to transverse modulation

- $\beta > \frac{\omega}{kv_a} \approx 1$ for small k : the instability is **ABSOLUTE**
i.e. **develops in time.**

possibly affected by kinetic effects

- $\beta < \frac{\omega}{kv_a} \approx 1$ for small k : the instability is **CONVECTIVE**
i.e. **develops along the direction of propagation.**

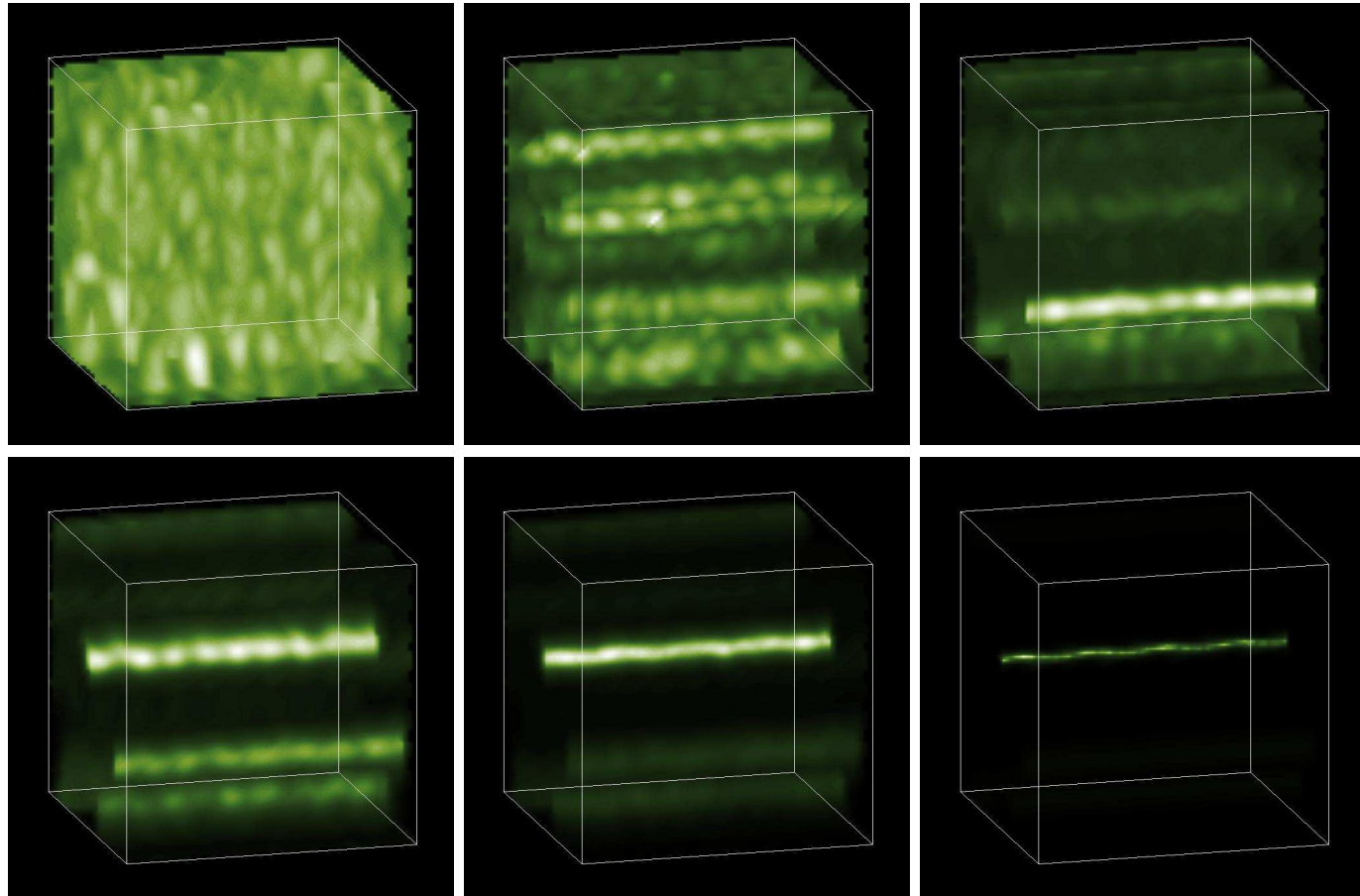


Figure 11: Formation of magnetic filaments.

What happens at later time?

The dynamics at longer times was addressed using a finite difference scheme with **adaptive mesh refinement** to reproduce a strong filamentation regime (*Dreher et al., Phys. Plasmas*, **12**, 052319 (2005)).

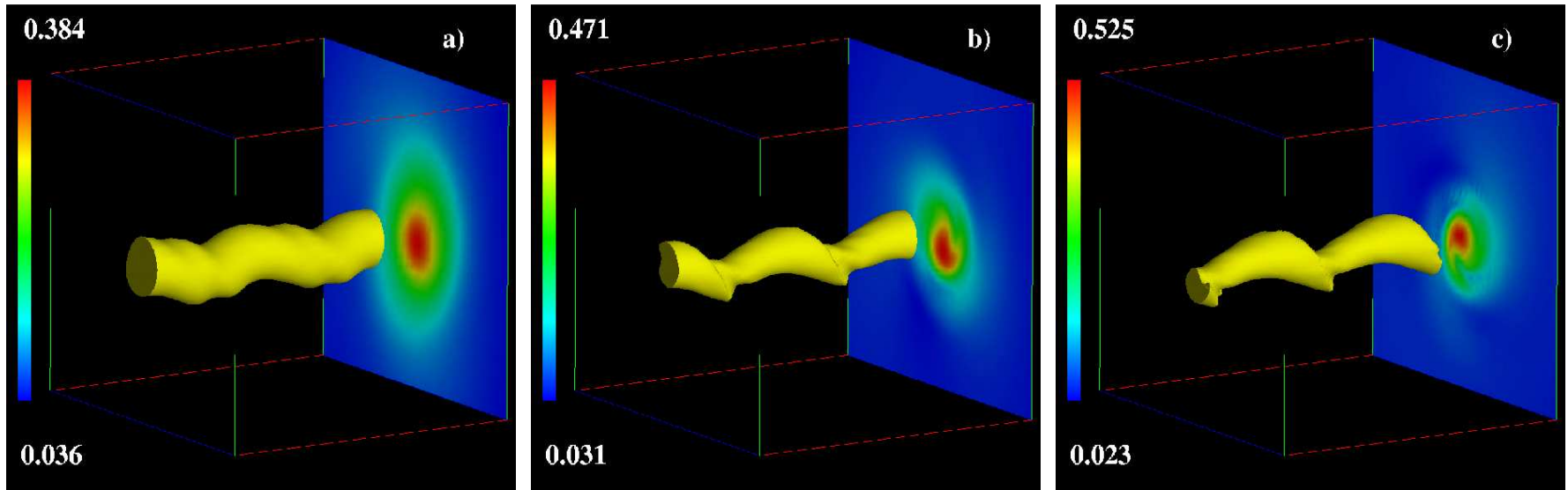


Figure 12: Isosurface of $|\mathbf{b}_\perp|$ at 75% of the maximum value and its transverse section at $x = 0$ for $t = 653.3$ (a), $t = 665.5$ (b), and $t = 667.6$ (c)

Strong distortion of the early-time cylindrical filaments: flattening and twisting of the structures.

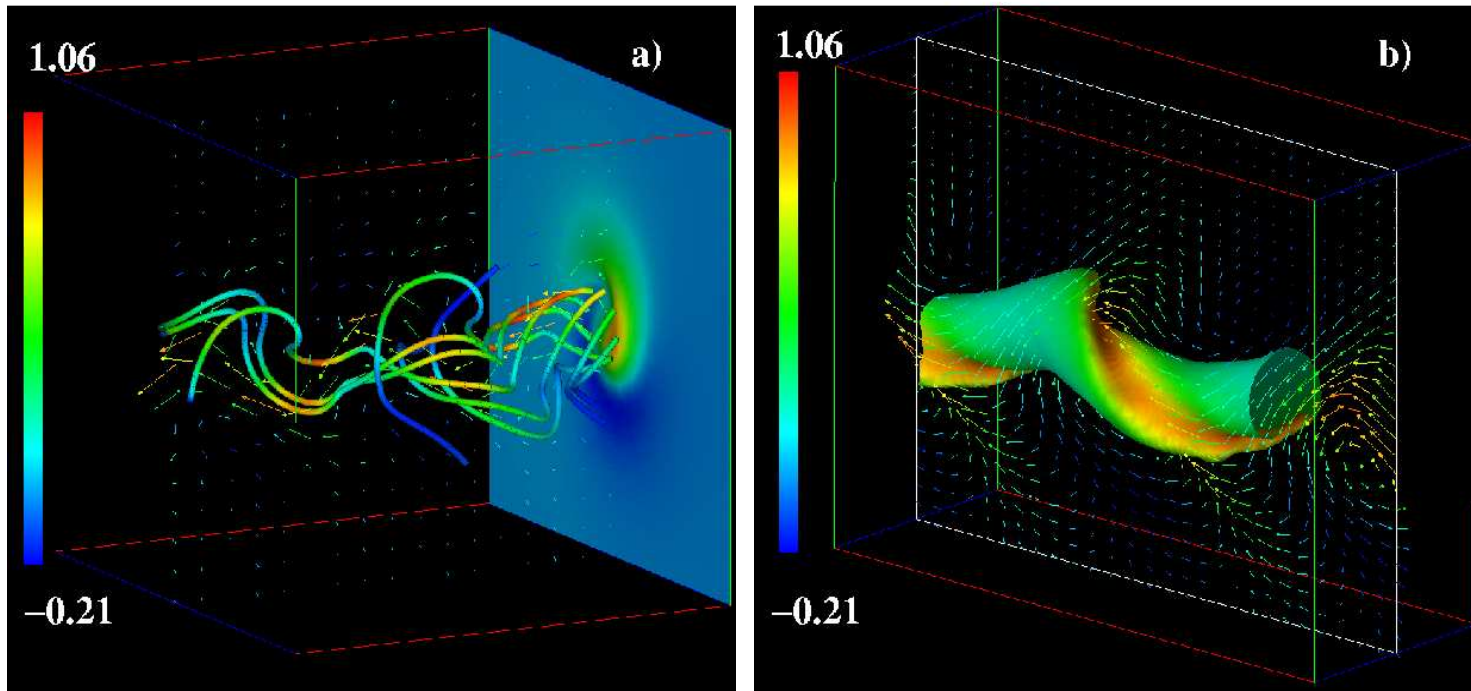


Figure 13: (a) Streamlines together with transverse cut for the longitudinal velocity; (b) Isosurface $|\mathbf{b}_\perp| = 0.35$ with plasma velocity arrows in a transverse plane at $t = 665.5$. Color code in both panels refers to u_x .

Transition from nonlinear waves to a hydrodynamic regime, characterized by intense current sheets and a strong acceleration of the plasma.

Filamentation in collisionless plasmas

Derive an envelope equation from the Landau fluid:

Define slow transverse variables $Y = \varepsilon\eta$ and $Z = \varepsilon\zeta$ and slow time $T = \varepsilon^2\tau$;

Consider a circularly polarized quasi-monochromatic Alfvén wave train, slowly modulated in the transverse directions: $b_{\perp} = (b_y, b_z)$; $b_y + ib_z = \varepsilon\psi(Y, Z, T)e^{i(k\xi - \omega\tau)}$.

The wave envelope obeys a **nonlinear Schrödinger equation with dissipation**

$$i\partial_T\psi + (\chi + i\nu)\Delta_{\perp}\psi + |\psi|^2\psi = 0$$

In collisionless plasmas, filamentation can take place for β significantly smaller than the critical value $\beta = 1$ provided by Hall-MHD.

The range of existence of the instability is in general enlarged as the ratio of electron to ion temperatures and/or the electron anisotropy are increased.

- When $T_{\perp} = T_{\parallel}$ for both ions and electrons with $T_i = T_e$: No filamentation instability
- When $T_{\perp} = T_{\parallel}$ for both ions and electrons with $T_i \ll T_e$, instability condition of the fluid theory is recovered.

Perspectives

- Benchmark the model by comparison with Vlasov-Maxwell, gyrokinetic, PIC and/or hybrid simulations.
- For mirror modes: develop a more refined model by closing at a higher order in the fluid hierarchy to get rid of close to isothermality assumption.
- Explore the nonlinear stage of parametric and mirror instabilities and in particular the formation of coherent structures and turbulent cascades.
- Simulation of 2D and 3D dispersive Alfvén and mirror wave turbulence
- Explore the possible description of nonlinear Landau damping.

References:

T. Chust & G. Belmont

- Closure of fluid equations in collisionless magnetoplasmas, submitted to PoP.

T. Passot & P.L. Sulem

- A long-wave model for Alfvén wave trains in a collisionless plasma:

I. Kinetic theory, *Phys. Plasmas* **10**, 3887 (2003).

II. A Landau-fluid approach, *Phys. Plasmas* **10**, 3906 (2003).

- Filamentation instability of long Alfvén waves in warm collisionless plasmas, *Phys. Plasmas* **10**, 3914 (2003).

- A fluid description for Landau damping of dispersive MHD waves, *Nonlinear Proc. Geophys.* **11**, 245 (2004).

- A Landau fluid model for dispersive magnetohydrodynamics, *Phys. Plasmas*, **11**, 5173 (2004).

- Towards fluid simulations of dispersive MHD waves in a warm collisionless plasma, in “Dynamical Processes in Critical Regions of the Heliosphere”, R. von Steiger and M. Gedalin eds., *Adv. Space Res.*, in press (with G. Bugnon).

- Landau-fluid simulations of Alfvén-wave instabilities in a warm collisionless plasma, *Nonlinear Proc. Geophys.*, **11**, 609 (2004) (with G. Bugnon).

- A Landau fluid model for warm collisionless plasmas, *Phys. Plasmas*, in press (with P. Goswami).

- A Landau fluid model for mirror mode turbulence, submitted to *JGR*.

Web site: <http://www.obs-nice.fr/passot/filamentation/AWfil.html>